

A Bayesian latent Gaussian conditional autoregressive copula model for analyzing spatially-varying trends in rainfall

Sayan Bhowmik and Arnab Hazra

Department of Mathematics and Statistics, Indian Institute of Technology Kanpur, Kanpur, 208016, India.

*Corresponding author(s). E-mail(s): ahazra@iitk.ac.in;
Contributing authors: sayanb22@iitk.ac.in;

Abstract

Assessing the availability of rainfall water plays a crucial role in rainfed agriculture. Given the substantial proportion of agricultural practices in India being rainfed and considering the potential trends in rainfall amounts across years due to climate change, we build a statistical model for analyzing annual total rainfall data for 34 meteorological subdivisions of mainland India available for 1951–2014. Here, we model the margins using a gamma regression model and the dependence through a Gaussian conditional autoregressive (CAR) copula model. Due to the natural variation of the average annual rainfall received across various dry through wet regions of the country, we allow areally-varying gamma regression coefficients under a latent Gaussian model framework. The neighborhood structure of the regions determines the dependence structure of both the likelihood and the prior layers, where we explore both CAR and intrinsic CAR structures for the priors. The proposed methodology also imputes the missing data effectively. We use the Markov chain Monte Carlo algorithms to draw Bayesian inferences. In simulation studies, the proposed model outperforms some competitors that do not allow a dependence structure at the data or prior layers. Implementing the proposed method for the Indian areal rainfall dataset, we draw inferences about the model parameters and discuss the potential effect of climate change on rainfall across India.

Keywords: Bayesian latent Gaussian model; Climate change; Gamma regression; Gaussian conditional autoregressive copula; Markov chain Monte Carlo; Rainfall modeling.

1 Introduction

Rainfall is a critical climatic factor influencing various sectors, including agriculture, hydrology, and disaster management. It is essential to analyze and model the spatial and temporal variations in rainfall, especially in monsoon-driven regions like India; with more than 60% of its agricultural land reliant on rainfed farming, India has the most considerable such extent globally [1, 2]. Climate change has intensified these uncertainties in recent decades, highlighting the need for statistical models that effectively capture rainfall patterns and dependencies [3]. Climate change alters weather patterns, and these shifts influence the distribution of temperature, wind, and rainfall, leading to variations in spatial rainfall patterns. While some regions may experience increased and more frequent rainfall, others may face droughts and declining precipitation. With varying marginal behavior across different global regions, rainfall exhibits inherent spatial dependence, shaped by large-scale atmospheric circulation, geographical features, and local climatic conditions [4, 5]. Hence, these phenomena motivate us to study varying trends in rainfall across the meteorological subdivisions of India while allowing a realistic spatial dependence structure exhibited by the data.

Historically, the statistical modeling of monthly, seasonal, or annual total rainfall has remained an important research area in meteorology. Annual total rainfall data are usually nonzero, and the histograms appear positively skewed; for all meteorological subdivisions of India, the recorded annual total rainfall data do not include any year with entirely nil rainfall. Hence, the justified probability distributions here are right-skewed and supported over the positive real line; some examples are exponential [6, 7], gamma [8, 9], log-normal [10, 11], Weibull [12, 13], and generalized exponential [14, 15] distributions. However, meteorologists have historically favored the gamma distribution for modeling rainfall data [16]. While the data across years are often assumed to be distributed identically in the meteorology literature, it is more appropriate to consider a nonstationary behavior across years in the marginal distribution due to the potential trends in meteorological variables driven by climate change. For this purpose, a gamma regression model is a possible approach that various researchers have explored for different scientific disciplines [17, 18].

While the gamma regression can effectively model the nonstationary marginal behavior in rainfall, a fundamental limitation of many traditional univariate models is their failure to incorporate spatial dependency, which is critical for accurate estimation and prediction [19]. Copulas [20–22] are powerful statistical tools that enable the modeling of complex dependencies between multiple random variables, even extending beyond traditional linear correlation measures [23, 24]. In spatial statistics, copulas facilitate the construction of joint distributions by separately modeling marginal distributions and their spatial dependence structure [25, 26]; this separation allows for greater flexibility in capturing nonlinear and asymmetric dependencies that are often present in spatial data, leading to improved inference and prediction in various applications [27–30]. [31] attempt to combine the copula theory with the entropy theory for bivariate rainfall and runoff analysis. Some other applications of copulas, e.g., Archimedean copulas for meteorological data, are covered in [32, 33]. [34] predict temporal trends of precipitation and temperature using copula under a climate change scenario. In our context of areal data, [35] propose a copula-based hierarchical model

with covariance selection for unbiased estimation of marginal parameters, providing a dependence structure with intuitive conditional and marginal interpretations. They develop a computational framework that permits efficient frequentist inference for their model, even for large datasets.

Several studies have demonstrated the efficacy of using gamma marginal distributions combined with copula models to analyze rainfall patterns. For instance, [36] employ gamma distributions as marginals within different copula models to capture spatial dependencies in precipitation data. On the other hand, [37] introduces a simulation-based method to enhance the preservation of cross-correlations in multisite precipitation simulations, addressing limitations observed in direct and indirect estimation methods. Here, the author explores a Gaussian copula with identical gamma marginal distributions for data collected at twelve nearby spatial locations; however, the model assumptions are unsuitable for a large geographical domain. Similarly, [38] utilize copulas with gamma marginal distributions to model the relationship between coarse- and fine-scale rainfall depths. The study in [39] describes precipitation intensity using space and time-dependent gamma distributions. While most of these researches do not assume a gamma regression framework for the margins, the rest do not focus on annual trends. Besides, the copulas used in these papers are for continuous spatial processes; hence, they are not directly applicable to areal data modeling.

Outside the avenue of copula-based modeling, the two most popular frameworks for areal data modeling are conditional autoregressive (CAR) models [40] and simultaneous autoregressive (SAR) models [41]. While SAR models are used widely in econometrics, regional science, and social sciences, CAR models are popular in Bayesian spatial statistics, epidemiology, and environmental studies. Among numerous uses of the CAR model in the environmental statistics literature, [42] use hierarchical CAR models for temperature variability analysis, [43] analyze flood risks and rainfall patterns using CAR models, and [44] use integrated CAR models with spatial dynamic processes for environmental prediction. In most of these models, the data are assumed to be Gaussian, conditioning on the parameters and the latent variables. However, using the CAR model as a copula in the context of environmental statistics or other scientific disciplines is not known.

Given the large spatial extent of the meteorological subdivisions of India, with some subdivisions in the western parts of the country receiving very low rainfall and some subdivisions in the east covering the wettest locations of the globe, the requirement of areally-varying gamma regression coefficients is obvious [45]. Besides, the regression coefficients are likely to express local homogeneity, and hence, we can model the priors for the areally-varying coefficients under the framework of Gaussian graphical models [42]. The CAR and intrinsic CAR [ICAR, 46] priors are popular choices for areally-varying coefficients. While [44] discuss ICAR priors in spatio-temporal ecological models, [42] use ICAR priors for modeling spatial rainfall variability. [47], [48], and many others use the CAR priors, while the R package `CARBayes` [49] implements some Bayesian areal data models with CAR priors.

In this paper, we develop a statistical model to analyze annual total rainfall data for 34 meteorological subdivisions of mainland India from 1951 to 2014. Given the suitability of the gamma distribution for modeling rainfall data and the possible

trend in the marginal distribution due to climate change, we assume a gamma regression model for the marginal distributions, where we consider a logarithmic link for the mean structure, written as a linear function of the years (suitably centered and scaled). We consider a Gaussian conditional autoregressive (CAR) copula for modeling the dependence structure where the adjacency is determined by whether or not two meteorological subdivisions share a boundary. While the usual CAR models show nonstationary marginal distributions due to the boundary effects, we appropriately scale the CAR covariance matrix to ensure the copula conditions are satisfied. We allow varying gamma regression coefficients within a latent Gaussian model framework to account for the natural variation in average annual rainfall across different climatic regions. Similar to the likelihood layer, the neighborhood structure of the regions determines the dependence structure in prior layers, where we explore CAR and ICAR priors. Our methodology also effectively imputes missing data. We draw Bayesian inference using Markov chain Monte Carlo algorithms, specifically, using a Metropolis-within-Gibbs sampler. To explore the benefit of considering the dependence structures at the likelihood and prior layers, we conduct an extensive simulation study by simulating many datasets of the same dimension as the Indian subdivision-wise rainfall dataset after assuming moderate through high spatial correlation. Using various criteria for model comparison, we then compare the performances of the proposed and competing models in terms of model fitting and estimation uncertainties. Applying this method to the Indian areal rainfall dataset, we draw inferences about the model parameters and examine the potential impacts of climate change on rainfall patterns across India.

We structure the remainder of this article as follows. Section 2 provides a brief background on gamma regression, conditional autoregressive models, and copulas. In Section 3, we describe the details of the Indian rainfall dataset we analyze and provide an exploratory analysis motivating us to choose specific components in the proposed statistical methodology. Section 4 details the construction of the conditional autoregressive copula for modeling spatial dependence, a gamma regression with areally-varying coefficients for margins, and the CAR and ICAR prior structures for the coefficients. In Section 5, we discuss an MCMC sampling strategy employed for parameter estimation. Section 6 discusses a simulation study to validate the correctness of the proposed parameter estimation procedure and to compare the proposed model with some simpler alternatives that ignore spatial dependence structures. In Section 7, we apply the proposed and competing methods to the Indian rainfall dataset and discuss the results. Finally, Section 8 concludes with a discussion on key findings, implications for climate studies, and future research directions.

2 Background

This section briefly overviews some key statistical tools required for our methodology and data analysis, including gamma regression for handling nonstationary skewed positive-valued data, conditional autoregressive (CAR) models for areal datasets, and copula. We also discuss two exploratory tools, including the Quantile-Quantile (QQ) plot of uniform-transformed data for marginal model validation and Moran’s I for

spatial autocorrelation assessment. Finally, we mention the Deviance information criterion (DIC) and the Watanabe-Akaike information criterion (WAIC) for Bayesian model comparison.

2.1 Gamma regression

In a gamma regression model for n independent but non-identically distributed positive-valued observations, we assume that the response variable Y_i follows

$$Y_i \stackrel{\text{Indep}}{\sim} \text{Gamma}(\mu_i, a), \quad i = 1, \dots, n, \quad (1)$$

where μ_i and a represent the mean and shape parameter, respectively. The density of the gamma distribution in (1) is given by

$$f(y_i) = \frac{(a/\mu_i)^a}{\Gamma(a)} y_i^{a-1} \exp[-ay_i/\mu_i], \quad y_i > 0, \mu_i > 0, a > 0.$$

The relationship between μ_i and covariates \mathbf{x}_i is modeled through a log-link function

$$\log(\mu_i) = \mathbf{x}_i^\top \boldsymbol{\beta}, \quad i = 1, \dots, n, \quad (2)$$

where $\boldsymbol{\beta}$ denotes the regression coefficients. This framework makes the marginal variance $\text{Var}(Y_i) = \mu_i^2/a \propto \mu_i^2$. Here, the rate parameter can be calculated as

$$\lambda_i = a/\mu_i = a \exp[-\mathbf{x}_i^\top \boldsymbol{\beta}] = \exp[\log(a) - \mathbf{x}_i^\top \boldsymbol{\beta}].$$

Here, the coefficient of variation $\sqrt{\text{Var}(Y_i)}/E(Y_i) = a^{-1/2}$ does not depend on μ_i .

2.2 Conditional Autoregressive (CAR) model

The CAR model assumes that the conditional distribution of the response variable at each region, given all other areas, depends only on the responses of the neighboring areas. Given a set of regionally indexed observations, the CAR model specifies a (zero-mean) Gaussian Markov Random Field (GMRF) structure

$$Y_i | Y_j, j \neq i \sim \text{Normal} \left(\rho \sum_{j \sim i} w_{ij} Y_j, \frac{\sigma^2}{m_i} \right), \quad (3)$$

where w_{ij} are spatial weights defining the neighborhood structure, ρ is the spatial autocorrelation parameter, and $m_i = \sum_{j \sim i} w_{ij}$. Using Brook's lemma [50], the covariance matrix for all regions is given by $\sigma^2(\mathbf{M} - \rho\mathbf{W})^{-1}$, where \mathbf{W} is the spatial weight matrix. The most common choice of w_{ij} s, the (i, j) th element of \mathbf{W} , is

$$w_{ij} = \begin{cases} 1 & \text{if } i \sim j \\ 0 & \text{if } i \not\sim j \end{cases}, \quad (4)$$

where $i \sim j$ indicates regions i and j are neighbors. Here, $i \approx i$, that is $w_{ii} = 0$ for all i . The correlation parameter ρ controls the strength of dependence among the regions. Here, \mathbf{M} is a diagonal matrix with its (i, i) th element $m_{ii} = \sum_j w_{ij}$, and σ^2 is a marginal variance parameter that controls the overall spatial covariance. The CAR models enable local spatial smoothing, ensuring that geographically close observations share information, thereby improving predictive accuracy and inference. Multiple types of CAR models are considered based on the situation. A proper CAR model is given in (3). When $\rho = 1$, the corresponding CAR model is called an intrinsic CAR (ICAR) model. The covariance matrix is singular for an ICAR model and hence, it can only be used as improper priors for areally-varying coefficients but not for modeling the likelihood.

2.3 Copulas

Copulas provide a flexible approach to modeling and estimating the joint distribution of variables independently of their marginal distributions, making them useful for capturing complex dependencies. A copula is a joint probability distribution function that ensures both marginal distributions are Uniform(0, 1). Specifically, a function $C(y_1, y_2)$ qualifies as a copula if $C(0, 0) = 0$ and for $y_1, y_2 \in (0, 1)$, it satisfies $C(y_1, 1) = y_1$, $C(1, y_2) = y_2$. Suppose we aim to determine a suitable joint probability distribution function $H(y_1, y_2)$ for random variables Y_1 and Y_2 , given that their marginal distributions follow the continuous distribution functions F_1 and F_2 , respectively. That is, given $F_1(y_1)$ and $F_2(y_2)$, along with knowledge of the dependency structure between Y_1 and Y_2 , we seek to define an appropriate joint distribution function as $H(y_1, y_2) = P(Y_1 \leq y_1, Y_2 \leq y_2)$. Since the transformed variables $U_1 = F_1(Y_1)$ and $U_2 = F_2(Y_2)$ follow a uniform distribution on $(0, 1)$, the joint distribution function of U_1 and U_2 forms a copula. Then

$$\begin{aligned} H(y_1, y_2) &= P(Y_1 \leq y_1, Y_2 \leq y_2) \\ &= P(F_1(Y_1) \leq F_1(y_1), F_2(Y_2) \leq F_2(y_2)) = C(F_1(y_1), F_2(y_2)). \end{aligned} \quad (5)$$

In our context, we consider a random vector following a standard bivariate Gaussian distribution with correlation ρ . The Gaussian copula function is defined as $C_\rho(u, v) = \Phi_\rho(\Phi^{-1}(u), \Phi^{-1}(v))$, where $u, v \in [0, 1]$, $\Phi(\cdot)$ represents the standard normal cumulative distribution function (CDF), and $\Phi_\rho(\cdot, \cdot)$ denotes the CDF of a standard bivariate Gaussian distribution with correlation ρ . To construct a bivariate Gamma distribution, we assume that the random vector (Y_1, Y_2) has gamma-distributed marginals given by the distribution functions F_1 and F_2 , respectively. Using the Gaussian copula, we define $(Y_1, Y_2) = (F_1^{-1}(\Phi(X_1)), F_2^{-1}(\Phi(X_2)))$, where F_1^{-1} and F_2^{-1} are the marginal quantile functions for Y_1 and Y_2 , and $(X_1, X_2) \sim \Phi_\rho$. The joint CDF of Y_1 and Y_2 is then given by $H(Y_1, Y_2; \rho) = C_\rho(\Phi(X_1), \Phi(X_2))$, while ensuring that the marginal distributions of Y_1 and Y_2 remain F_1 and F_2 , respectively.

An appropriate copula should accurately represent the assumed dependencies between U_1 and U_2 . Since F_1 and F_2 are increasing functions, the dependence structure induced by the chosen copula should reflect the relationship we expect between Y_1 and Y_2 . For example, if we assume that Y_1 and Y_2 have a correlation of ρ , we should

select a copula such that the random variables following this copula exhibit a correlation of ρ . However, since correlation captures only linear dependencies, the correlation between Y_1 and Y_2 does not necessarily match the correlation between U_1 and U_2 [51].

2.4 Uniform-transformed Quantile-Quantile (QQ) plot

Model validation is essential to ensure the reliability of statistical inference. Suppose we are interested in fitting a marginal distribution model $F(\cdot, \theta_i)$ where θ_i denotes the model parameter corresponding to the i th observation Y_i and possibly different across observations that we can simplify in terms of some covariates under a regression model setup. Based on some estimates of θ_i , say $\hat{\theta}_i$, approximately $Y_i \sim F(\cdot, \hat{\theta}_i)$ and thus $F(Y_i, \hat{\theta}_i) \sim \text{Uniform}(0, 1)$ if the model F is appropriate. We can thus consider a QQ plot of low through high quantiles of the $\text{Uniform}(0, 1)$ distribution and the corresponding quantiles of the empirical CDF of $F(Y_i, \hat{\theta}_i)$ s as a diagnostic tool. We call this tool a Uniform-transformed QQ plot [52]. If the plot remains close to the $y = x$ line, we can safely consider F a reasonable model. If we compare two models, F_1 and F_2 , we can calculate and compare the uniformed-transformed QQ plots for both distributions. While we can use a Kolmogorov-Smirnov test for a similar purpose, the uniformed-transformed QQ plots showcase the range of quantiles where the model fitting is reasonable; for example, a model may fit the data distribution well in the bulk and poorly in the tails, and this tool can explain the scenario.

2.5 Moran’s I for assessing spatial autocorrelation

Areal data often exhibit autocorrelation, meaning that observations at nearby, possibly neighboring, regions are more similar than distant ones. Moran’s I [53] is a widely used measure for detecting spatial autocorrelation, and it is calculated as

$$I = \frac{N}{\sum_i \sum_j w_{ij}} \times \frac{\sum_i \sum_j w_{ij} (Y_i - \bar{Y})(Y_j - \bar{Y})}{\sum_i (Y_i - \bar{Y})^2}, \quad (6)$$

where Y_i represents the observed value at region i , w_{ij} is the spatial weight matrix defining neighborhood relationships in (4), \bar{Y} is the mean value of Y_i , and N is the total number of locations. Moran’s I ranges from -1 to $+1$, where positive values of Moran’s I suggest clustering, negative values indicate dispersion, and values near zero suggest spatial randomness. Under the null hypothesis of complete randomness, $E(I) = -1/(N - 1)$ and $\text{Var}(I)$ can be calculated in terms of w_{ij} s, and we thus can obtain a z -score by centering and scaling. Finally, we obtain the p -value by assuming normality for the test statistic and decide on the spatial randomness accordingly.

2.6 Bayesian model comparison

To compare multiple Bayesian models with the same likelihood structure but different prior structures, we report Deviance information criteria [DIC, 54] and Watanabe-Akaike information criteria [WAIC, 55]. We calculate DIC as

$$\text{DIC} = \bar{D} + p_D = D(\mathbf{Y} | \hat{\theta}) + 2p_D,$$

where $D(\mathbf{Y}|\boldsymbol{\theta}) = -2\log[p(\mathbf{Y}|\boldsymbol{\theta})]$ is the deviance for measuring model fit, \bar{D} is the posterior mean deviance defined as $E(D(\mathbf{Y}|\boldsymbol{\theta})|\mathbf{Y})$, $\hat{\boldsymbol{\theta}} = E(\boldsymbol{\theta}|\mathbf{Y})$ is the posterior mean of the model parameter vector $\boldsymbol{\theta}$, and $p_D = \bar{D} - D(\mathbf{Y}|\hat{\boldsymbol{\theta}})$ is the effective number of parameters in the model. Given the MCMC outputs, calculating DIC is straightforward. The intuition is that models with smaller DIC are parsimonious (small p_D) and fit well (small \bar{D}).

Further, we can compute WAIC, also known as the widely applicable information criteria, as an alternative to DIC. Here, WAIC approximates n -fold (i.e., leave-one-out) cross-validation. Suppose we have n independent observations (possibly vectors) \mathbf{Y}_i for $i = 1, \dots, n$ and $\boldsymbol{\theta}$ is the parameter vector in the model (likelihood) $f(\cdot)$. Let m_i and v_i be the posterior mean and variance of $\log[f(\mathbf{Y}_i|\boldsymbol{\theta})]$. The effective model size is $p_W = \sum_{i=1}^n v_i$ and WAIC is given by

$$\text{WAIC} = -2 \sum_{i=1}^n m_i + 2p_W.$$

WAIC estimates complexity based on the variance of the log-likelihood across posterior samples; this accounts for models with hierarchical structures or non-Gaussian posteriors where the parameter count is ambiguous.

The measure DIC is computationally simpler than WAIC but may be unreliable for hierarchical and complex models. At the same time, WAIC is more general and provides a better approximation of predictive performance, making it preferable in most Bayesian applications. [56] recommend using WAIC or leave-one-out cross-validation over DIC for model comparison in modern Bayesian workflows.

3 Data description and exploratory analysis

Unlike the administrative state-wise boundaries, mainland India (excluding Andaman and Nicobar Islands and Lakshadweep Archipelago) comprises 34 meteorological subdivisions; the division is determined based on meteorological homogeneity [4]. We present the geographical boundaries of these 34 subdivisions in Figure 2. We obtain annual total rainfall data (in mm) for these subdivisions, covering the years 1951 to 2014, from the Open Government Data (OGD) Platform, India (<https://data.gov.in>), along with shape files of the boundaries. Based on the rainfall data collected from 641 districts across India by the India Meteorological Department (IMD), [4] computed monthly rainfall amounts for these districts by averaging the rainfall data from available stations within each district for each month. An area-weighted averaging method was then applied to derive subdivision-wise rainfall data from the district-wise data. [57] provide a more detailed report on the dataset preparation. The rest of the paper focuses on analyzing this dataset, which we refer to as the ‘‘Indian rainfall dataset’’.

Suppose we denote the annual total rainfall for the i th meteorological subdivision and t th year by Y_{it} , for $i = 1, \dots, n$ and $t = 1, \dots, T$ with $n = 34$ and $T = 64$. Given the extensive 64-year observational period encompassing phases of global warming, significant trends across the years are plausible. The data are positive-valued; hence, we can model the marginal distributions using log-normal or gamma regression, for

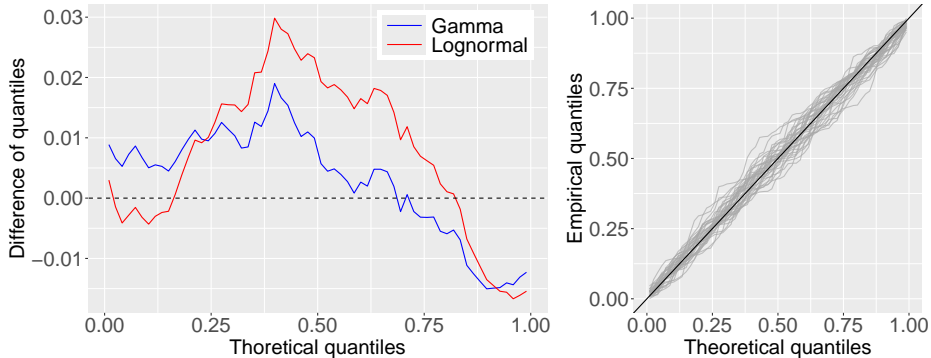


Fig. 1: Left: Difference between the uniform transformed data-quantiles and Uniform(0, 1) quantiles for the fitted gamma and lognormal regression models after combining all subdivisions. Here, a model is preferred over the other if the difference in quantiles remains nearer to zero (the dashed line); Right: Q-Q plots of the uniform-transformed data quantiles when the marginal distributions are gamma for 34 meteorological subdivisions of mainland India.

example, where we can model the mean as a function of the year. A log-normal distribution assumption is more popular in general spatial or areal data analysis literature because we can consider a logarithmic transformation of the data and model them using an ordinary or spatial linear regression framework instead of a generalized ordinary or spatial linear regression framework. At the same time, as mentioned in Section 1, the gamma distribution assumption for the margins is the most popular in rainfall modeling literature.

We first postulate that the data are independently distributed across years and marginally follow a gamma distribution. To model the space-time varying mean parameter, we write $E(Y_{it}) = \mu_{it}$ with areally-varying shape parameter α_i . Hence, for every region index i , we assume

$$Y_{it} \stackrel{\text{ind}}{\sim} \text{Gamma}(\mu_{it}, \alpha_i), \quad t = 1, \dots, T, \quad (7)$$

where α_i is the shape parameter and μ_{it} is the mean of the gamma distribution for region index i and time point t , which is connected with a log-link function

$$\log(\mu_{it}) = \alpha_i + \beta_i t, \quad t = 1, \dots, T, \quad (8)$$

in which α_i and β_i are areally-varying coefficients. A competing log-normal model would be $Y_{it}^* = \log(Y_{it}) \stackrel{\text{ind}}{\sim} \text{Normal}(\mu_{it}, \sigma_i^2)$, $t = 1, \dots, T$, where $\mu_{it} = \alpha_i^* + \beta_i^* t$ for some areally-varying coefficients α_i^* , β_i^* , and variances σ_i^2 . We separately fit the regression models for every region index i using maximum likelihood estimates and compare their uniform-transformed QQ plots in the left panel of Figure 1. The log-normal model better fits low quantile levels, while the gamma model outperforms the

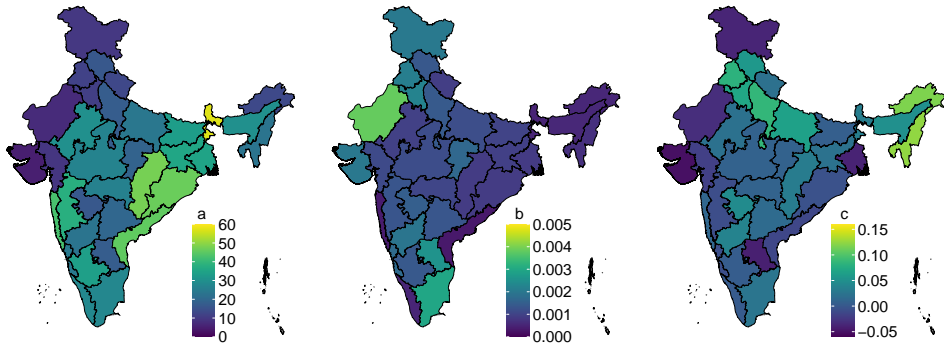


Fig. 2: MLEs of the parameter vectors \mathbf{a} (left), \mathbf{b} (middle), and \mathbf{c} (right) for 34 meteorological subdivisions of mainland India.

lognormal model overall. Compared to the lognormal model, the gamma model provides approximately 7% lower root mean square error and mean absolute error (in terms of fitting). For every subregion i , we present the uniform-transformed quantiles based on gamma regression in the right panel of Figure 1. Except for certain middle-range quantiles, the model fits the data reasonably well. In the rest of the paper, we subsequently consider the gamma model in (7) and (8).

We further reparameterize the model in (7) and (8) in terms of a standard representation of a gamma distribution using shape and rate parameters as follows. First we rewrite (8) as $\log(\mu_{it}) = \tilde{\alpha}_i + \tilde{\beta}_i t^*$, where $\tilde{\alpha}_i = \alpha_i + \beta_i m_t$, $\tilde{\beta}_i = \beta_i s_t$, and $t^* = (t - m_t)/s_t$ with $m_t = T^{-1} \sum_{t=1}^T t$ and $s_t^2 = T^{-1} \sum_{t=1}^T t^2 - m_t^2$. Then, following (7), the rate parameter is given by

$$\lambda_{it} = \frac{a_i}{\mu_{it}} = a_i \exp[-\tilde{\alpha}_i] \exp[-\tilde{\beta}_i t^*] = a_i b_i \exp[c_i t^*], \quad (9)$$

where c_i , the coefficient of t^* , captures the climate change behavior over the years for the meteorological subdivision i . In this parameterization, the mean and variance of Y_{it} can be obtained as

$$\begin{aligned} E(Y_{it}) &= \mu_{it} = \frac{a_i}{\lambda_{it}} = \frac{a_i}{a_i b_i \exp[c_i t^*]} = b_i^{-1} \exp[-c_i t^*] = \exp[\alpha_i + \beta_i t], \\ \text{Var}(Y_{it}) &= \frac{a_i}{\lambda_{it}^2} = \frac{a_i}{a_i^2 b_i^2 \exp[2c_i t^*]} = \frac{1}{a_i} (b_i^{-1} \exp[-c_i t^*])^2 = \frac{1}{a_i} \mu_{it}^2. \end{aligned} \quad (10)$$

Here, the coefficient of variation, $a_i^{-1/2}$ for region i , remains constant over t . We further interpret a_i as a shape parameter, b_i as an intercept-related parameter, and c_i as a slope-related parameter; the rest of the paper follows this parameterization.

For exploratory analysis, we fit the model in (7) and (9) separately for every region i using maximum likelihood estimation procedure and we present the estimates (MLEs) of $\mathbf{a} = (a_1, \dots, a_n)^\top$, $\mathbf{b} = (b_1, \dots, b_n)^\top$ and $\mathbf{c} = (c_1, \dots, c_n)^\top$ in Figure 2. The standard errors of the estimates are low due to $T = 64$ replications used for the

analysis, and hence, any spatial pattern visible in Figure 2 can be conceptualized to build a flexible model for them. First, we notice that the MLEs of a_i s, b_i s, and c_i s are non-constant across space, motivating us to consider areally-varying coefficients. Second, the estimates for nearby regions exhibit similarity, indicating the suitability of a CAR or an ICAR prior for the parameters.

We further explore the requirement of a spatial modeling of the likelihood layer for the Indian rainfall dataset. Denoting the gamma CDF for region i by $F(\cdot; a_i, b_i, c_i)$ and the corresponding MLEs of the model parameters by \hat{a}_i , \hat{b}_i , and \hat{c}_i , and based on the suitability of the gamma distribution for the data, $F(Y_{it}; \hat{a}_i, \hat{b}_i, \hat{c}_i)$ follows a Uniform(0, 1) distribution (approximately). Thus, $\Phi^{-1}(F(Y_{it}; \hat{a}_i, \hat{b}_i, \hat{c}_i)) = X_{it}$ (say) follows a Normal(0, 1) distribution (approximately, where $\Phi^{-1}(\cdot)$ is the standard normal quantile function) and we can assess the spatial dependence in Y_{it} s via the Moran's I of X_{it} s. We obtain the average (over t) Moran's I to be 0.3613 with a negligible p -value, indicating a significant positive spatial association; this motivates us to choose a CAR model for the likelihood.

4 Methodology

In this section, we discuss our proposed Bayesian hierarchical model. We first discuss a CAR copula model and then develop the model layers using the copula.

4.1 CAR copula

Let $\tilde{\mathbf{X}} = (\tilde{X}_1, \dots, \tilde{X}_n)'$ be a random vector following a CAR model defined in Section 2.2, where the adjacency matrix is constructed using the neighborhood structure of the meteorological subdivisions of mainland India. Given the spatial autocorrelation parameter ρ and fixed unit marginal variance ($\sigma^2 = 1$), the joint distribution of $\tilde{\mathbf{X}}$ is given by $\tilde{\mathbf{X}} \sim \text{Normal}_n(\mathbf{0}, [\mathbf{M} - \rho\mathbf{W}]^{-1})$, where \mathbf{M} and \mathbf{W} are as defined in Section 2.2 and Normal_n denotes an n -variate normal distribution. Suppose the diagonal elements of the matrix $[\mathbf{M} - \rho\mathbf{W}]^{-1}$ are given by d_i for $i = 1, \dots, n$ and $\mathbf{\Delta} = \text{diag}(d_1, \dots, d_n)$. Then, $\mathbf{\Delta}^{-1/2}\tilde{\mathbf{X}} \sim \text{Normal}_n(\mathbf{0}, \mathbf{\Delta}^{-1/2}[\mathbf{M} - \rho\mathbf{W}]^{-1}\mathbf{\Delta}^{-1/2})$ and its corresponding marginal distributions are Normal(0, 1). Denoting $U_i = \Phi(d_i^{-1/2}\tilde{X}_i)$ for $i = 1, \dots, n$, where $\Phi(\cdot)$ denotes the standard normal CDF, we call the joint distribution of $\mathbf{U} = (U_1, \dots, U_n)'$ a CAR copula with adjacency matrix \mathbf{W} and spatial autocorrelation parameter ρ . The joint CDF of \mathbf{U} is given by

$$C(u_1, \dots, u_n) = \Phi_n([\Phi^{-1}(u_1), \dots, \Phi^{-1}(u_n)]; \mathbf{0}, \mathbf{\Delta}^{-1/2}[\mathbf{M} - \rho\mathbf{W}]^{-1}\mathbf{\Delta}^{-1/2}),$$

where $\Phi_n(\cdot; \boldsymbol{\mu}, \boldsymbol{\Sigma})$ denotes the joint CDF of an n -dimensional multivariate normal distribution with mean vector $\boldsymbol{\mu}$ and covariance matrix $\boldsymbol{\Sigma}$. The corresponding copula density function is given by

$$c(u_1, \dots, u_n) = \frac{\phi_n([\Phi^{-1}(u_1), \dots, \Phi^{-1}(u_n)]; \mathbf{0}, \mathbf{\Delta}^{-1/2}[\mathbf{M} - \rho\mathbf{W}]^{-1}\mathbf{\Delta}^{-1/2})}{\prod_{i=1}^n \phi(\Phi^{-1}(u_i))},$$

where $\phi_n(\cdot; \boldsymbol{\mu}, \boldsymbol{\Sigma})$ denotes the joint density corresponding to $\Phi_n(\cdot; \boldsymbol{\mu}, \boldsymbol{\Sigma})$ and $\phi(\cdot)$ are standard normal densities.

4.2 Data layer modeling

We recall the data setup from Section 3, where the annual total rainfall data are denoted by Y_{it} for $i = 1, \dots, n = 34$ meteorological subdivisions of India and for $t = 1, \dots, T = 64$ years between 1951 and 2014.

We separately model the marginal distribution and dependence structure of Y_{it} s in the data layer. Following (7) and (9), given the marginal distribution-related parameters a_i , b_i , and c_i , the conditional distribution of Y_{it} is

$$Y_{it}|a_i, b_i, c_i \stackrel{\text{iid}}{\sim} \text{Gamma}(b_i^{-1} \exp[-c_i t^*], a_i), \quad t = 1, \dots, T, \quad (11)$$

where $t^* = (t - m_t)/s_t$ with $m_t = T^{-1} \sum_{t=1}^T t$ and $s_t^2 = T^{-1} \sum_{t=1}^T t^2 - m_t^2$. Henceforth, we denote the CDF of the gamma distribution in (11) as $F(\cdot; a_i, b_i, c_i)$. Thus, $U_{it} = F(Y_{it}; a_i, b_i, c_i) \sim \text{Uniform}(0, 1)$. Let the vectors of a_i s, b_i s, and c_i s be denoted by \mathbf{a} , \mathbf{b} , and \mathbf{c} , respectively, as described in Section 3. Conditioning on \mathbf{a} , \mathbf{b} , and \mathbf{c} , while we assume independence across years, we model the spatial dependence of $\mathbf{U}_t = (U_{1t}, \dots, U_{nt})'$ in a copula framework as described in Section 4.1. Overall, the density of $\mathbf{Y}_t = (Y_{1t}, \dots, Y_{nt})$ given \mathbf{a} , \mathbf{b} , \mathbf{c} , and ρ is

$$\begin{aligned} f_n(\mathbf{y}_t|\mathbf{a}, \mathbf{b}, \mathbf{c}, \rho) &= \phi_n([\Phi^{-1}(u_{1t}), \dots, \Phi^{-1}(u_{nt})]; \mathbf{0}, \boldsymbol{\Delta}^{-1/2}[\mathbf{M} - \rho\mathbf{W}]^{-1}\boldsymbol{\Delta}^{-1/2}) \\ &\quad \times \prod_{i=1}^n f(y_{it}; a_i, b_i, c_i) / \prod_{i=1}^n \phi(\Phi^{-1}(u_{it})) \quad , \end{aligned} \quad (12)$$

where $u_{it} = F(y_{it}; a_i, b_i, c_i)$, $f(y_{it}; a_i, b_i, c_i)$ denotes the density corresponding to the gamma distribution in (11). Further, assuming independence across time, the joint density of the full data is $f_n(\mathbf{y}_1, \dots, \mathbf{y}_T|\mathbf{a}, \mathbf{b}, \mathbf{c}, \rho) = \prod_{t=1}^T f_n(\mathbf{y}_t|\mathbf{a}, \mathbf{b}, \mathbf{c}, \rho)$.

4.3 Bayesian latent Gaussian model

In this subsection, we subsequently model the areally-varying coefficients a_i s, b_i s, and c_i s. The range of these coefficients are $a_i > 0, b_i > 0, c_i \in \mathbb{R}$. We thus consider the logarithmic transformation of the first two and define $a_i^* = \log(a_i)$ and $b_i^* = \log(b_i)$ and choose different dependent or independent Gaussian priors for them as follows.

Case 1. We assume independent and identically distributed (iid) Gaussian priors to the parameters as follows

$$\begin{aligned} a_i^*|\mu_a, \sigma_a^2 &\stackrel{\text{iid}}{\sim} \text{Normal}(\mu_a, \sigma_a^2), \\ b_i^*|\mu_b, \sigma_b^2 &\stackrel{\text{iid}}{\sim} \text{Normal}(\mu_b, \sigma_b^2), \\ c_i|\mu_c, \sigma_c^2 &\stackrel{\text{iid}}{\sim} \text{Normal}(\mu_c, \sigma_c^2), \end{aligned} \quad (13)$$

for all $i = 1, 2, \dots, n$. Here, μ_a and σ_a^2 represent the overall average of a_i^* s and spatial variability of a_i^* s considering mainland India. Similarly, μ_b and σ_b^2 represent the overall average of b_i^* s and spatial variability of b_i^* s, and μ_c and σ_c^2 represent the overall average of c_i s and spatial variability of c_i s. The prior choice in (13) does not allow a spatial dependence structure visible from Figure 2. Besides, the rainfall patterns of two neighboring regions usually behave similarly for natural climatic reasons. Hence, it is likely that (13) would underperform compared to a model that appropriately considers a spatial dependence structure, and the spatial smoothing of the parameters is controlled by the data only.

Case 2. Considering the potential geographical relationships of the rainfall pattern for two nearby meteorological subdivisions, we consider CAR prior specifications for the parameters as follows

$$\begin{aligned} \mathbf{a}^* &= (\log(a_1), \dots, \log(a_n))' \sim \text{Normal}_n(\mu_a \mathbf{1}, \sigma_a^2 [\mathbf{M} - \rho_a \mathbf{W}]^{-1}), \\ \mathbf{b}^* &= (\log(b_1), \dots, \log(b_n))' \sim \text{Normal}_n(\mu_b \mathbf{1}, \sigma_b^2 [\mathbf{M} - \rho_b \mathbf{W}]^{-1}), \\ \mathbf{c} &= (c_1, \dots, c_n)' \sim \text{Normal}_n(\mu_c \mathbf{1}, \sigma_c^2 [\mathbf{M} - \rho_c \mathbf{W}]^{-1}), \end{aligned} \quad (14)$$

where ρ_a, ρ_b , and ρ_c capture spatial autocorrelation of the parameters a_i s, b_i s, and c_i s. The other hyperparameters $\mu_a, \mu_b, \mu_c, \sigma_a^2, \sigma_b^2$, and σ_c^2 have similar meaning as in Case 1. The adjacency matrix is the same as in Section 4.2.

Case 3. While the spatial correlation structure in (14) is more general, estimating the hyperparameters ρ_a, ρ_b , and ρ_c is usually challenging due to high posterior uncertainty. Thus, as a special case, we consider Intrinsic CAR (ICAR) [58] prior specifications for the parameters as follows

$$\begin{aligned} \mathbf{a}^* &= (\log(a_1), \dots, \log(a_n))^\top \sim \text{Normal}_n(\mu_a \mathbf{1}, \sigma_a^2 [\mathbf{M} - \mathbf{W}]^{-1}), \\ \mathbf{b}^* &= (\log(b_1), \dots, \log(b_n))^\top \sim \text{Normal}_n(\mu_b \mathbf{1}, \sigma_b^2 [\mathbf{M} - \mathbf{W}]^{-1}), \\ \mathbf{c} &= (c_1, \dots, c_n)^\top \sim \text{Normal}_n(\mu_c \mathbf{1}, \sigma_c^2 [\mathbf{M} - \mathbf{W}]^{-1}), \end{aligned} \quad (15)$$

where we set $\rho_a = 1, \rho_b = 1$ and $\rho_c = 1$ in Case 2. While the priors are improper due to singular covariance matrices, their posteriors are proper, and hence, the inferences are reliable.

Finally, we choose a weakly-informative Uniform(0, 1) prior for ρ . For the hyperparameters, we again choose weakly-informative hyperpriors

$$\begin{aligned} \mu_a, \mu_b, \mu_c &\stackrel{\text{iid}}{\sim} \text{Normal}(0, 10^2), \\ \sigma_a^2, \sigma_b^2, \sigma_c^2 &\stackrel{\text{iid}}{\sim} \text{Inverse-gamma}(0.01, 0.01), \\ \rho_a, \rho_b, \rho_c &\stackrel{\text{iid}}{\sim} \text{Uniform}(0, 1). \end{aligned} \quad (16)$$

Altogether, (12), (14), and (16) specify a fully Bayesian hierarchical model, and we henceforth call it the CAR-CAR model due to a CAR structure at the both data and prior layers. Similarly, we call the model specified by (12), (15), and (16) (ignoring

the hyperpriors for ρ_a , ρ_b , and ρ_c) as CAR-ICAR model, and the model specified by (12), (15), and (16) as CAR-Indep model.

5 Bayesian computation

This section discusses the MCMC sampling steps for the CAR-CAR model. The sampling for the other models mentioned in the previous section can be done simply by ignoring some update steps. For example, the computation for the CAR-ICAR model can be done just by ignoring the updates of ρ_a , ρ_b , and ρ_c and setting them to one.

5.1 Gibbs sampling steps for the CAR-CAR model

The set of parameters and hyperparameters in the model are

$$\Theta = \{\mathbf{a}^*, \mathbf{b}^*, \mathbf{c}, \rho, \mu_a, \mu_b, \mu_c, \sigma_a^2, \sigma_b^2, \sigma_c^2, \rho_a, \rho_b, \rho_c, Y_{it}^*s\},$$

which includes some parameter vectors, and the rest are single parameters or hyperparameters. We update each of the vectors \mathbf{a}^* , \mathbf{b}^* , and \mathbf{c} simultaneously using a block MH algorithm. Here, by Y_{it}^*s , we denote the missing data that needs to be imputed within the MCMC steps. The update steps within a Gibbs sampler are as follows.

- **Updating \mathbf{a}^* :** Sample \mathbf{a}^* via Metropolis-Hasting algorithm from

$$\begin{aligned} & f(\mathbf{a}^* | \mathbf{Y}_1, \dots, \mathbf{Y}_T, \mathbf{b}^*, \mathbf{c}, \rho, \mu_a, \sigma_a^2, \rho_a) \\ & \propto \prod_{t=1}^T f_n(\mathbf{y}_t | \mathbf{a}, \mathbf{b}, \mathbf{c}, \rho) \times \phi_n(\mathbf{a}^*; \mu_a \mathbf{1}, \sigma_a^2 [\mathbf{M} - \rho_a \mathbf{W}]^{-1}), \end{aligned}$$

where f_n is given by (12), $a_i = \exp[a_i^*]$, $b_i = \exp[b_i^*]$ for $i = 1, \dots, n$, $\phi_n(\cdot; \boldsymbol{\mu}, \boldsymbol{\Sigma})$ is the multivariate normal density with mean vector $\boldsymbol{\mu}$ and covariance matrix $\boldsymbol{\Sigma}$.

- **Updating \mathbf{b}^* :** Similar to \mathbf{a}^* , sample \mathbf{b}^* jointly via Metropolis-Hasting algorithm from $f(\mathbf{b}^* | \mathbf{Y}_1, \dots, \mathbf{Y}_T, \mathbf{a}^*, \mathbf{c}, \rho, \mu_b, \sigma_b^2, \rho_b)$.
- **Updating \mathbf{c} :** Similar to \mathbf{a}^* , and \mathbf{b}^* , sample \mathbf{c} jointly via Metropolis-Hasting algorithm from $f(\mathbf{c} | \mathbf{Y}_1, \dots, \mathbf{Y}_T, \mathbf{a}^*, \mathbf{b}^*, \rho, \mu_c, \sigma_c^2, \rho_c)$.
- **Updating ρ :** Sample ρ via the Metropolis-Hasting algorithm from

$$\begin{aligned} & f(\rho | \mathbf{Y}_1, \dots, \mathbf{Y}_T, \mathbf{a}^*, \mathbf{b}^*, \mathbf{c}) \\ & \propto \prod_{t=1}^T \phi_n([\Phi^{-1}(U_{1t}), \dots, \Phi^{-1}(U_{nt})]; \mathbf{0}, \Delta^{-1/2} [\mathbf{M} - \rho \mathbf{W}]^{-1} \Delta^{-1/2}) \mathbb{1}(\rho \in (0, 1)), \end{aligned}$$

where $U_{it} = F(Y_{it}; a_i = \exp[a_i^*], b_i = \exp[b_i^*], c_i)$ with $F(\cdot; a, b, c)$ the CDF of a gamma distribution as described in (11), and $\mathbb{1}(\cdot)$ is an indicator.

- **Updating μ_a :** Sample μ_a directly from the full conditional distribution, which is

$$\mu_a | \mathbf{a}^*, \rho_a, \sigma_a^2 \sim \text{Normal} \left(\frac{\sigma_a^{-2} \mathbf{1}' [\mathbf{M} - \rho_a \mathbf{W}] \mathbf{a}^*}{\sigma_a^{-2} \mathbf{1}' [\mathbf{M} - \rho_a \mathbf{W}] \mathbf{1} + 10^{-2}}, \frac{1}{\sigma_a^{-2} \mathbf{1}' [\mathbf{M} - \rho_a \mathbf{W}] \mathbf{1} + 10^{-2}} \right).$$

- **Updating μ_b :** Similar to μ_a , update μ_b by sampling directly from the full conditional distribution $f(\mu_b|\mathbf{b}^*, \sigma_b^2, \rho_b)$.
- **Updating μ_c :** Similar to μ_a , update μ_c by sampling directly from the full conditional distribution $f(\mu_c|\mathbf{c}, \sigma_c^2, \rho_c)$.
- **Updating σ_a^2 :** Sample σ_a^2 directly from the full conditional distribution, which is

$$\sigma_a^2|\mathbf{a}^*, \mu_a, \rho_a \sim \text{Inverse-gamma}(0.5n + 0.01, 0.5(\mathbf{a}^* - \mu_a\mathbf{1})'[\mathbf{M} - \rho_a\mathbf{W}](\mathbf{a}^* - \mu_a\mathbf{1}) + 0.01)$$

- **Updating σ_b^2 :** Similar to σ_a^2 , update σ_b^2 by sampling directly from the full conditional distribution $f(\sigma_b^2|\mathbf{b}^*, \mu_b, \rho_b)$.
- **Updating σ_c^2 :** Similarly, update σ_c^2 by sampling directly from the full conditional distribution $f(\sigma_c^2|\mathbf{c}, \mu_c, \rho_c)$.
- **Updating ρ_a :** Sample ρ_a via the Metropolis-Hasting algorithm from

$$f(\rho_a|\mathbf{a}^*, \mu_a, \sigma_a^2) \propto \phi_n(\mathbf{a}^*; \mu_a\mathbf{1}, \sigma_a^2[\mathbf{M} - \rho_a\mathbf{W}]^{-1})\mathbb{1}(\rho_a \in (0, 1)).$$

- **Updating ρ_b :** Similarly, sample ρ_b from $f(\rho_b|\mathbf{b}^*, \mu_b, \sigma_b^2)$ via Metropolis-Hasting algorithm as ρ_a .
- **Updating ρ_c :** Similarly, sample ρ_c from $f(\rho_c|\mathbf{c}, \mu_c, \sigma_c^2)$ via Metropolis-Hasting algorithm as ρ_a and ρ_b .
- **Updating Y_{it}^* s:** For a time point t , if \mathcal{I} denotes the region indexes where the data are missing, we construct \mathbf{Y}_t^* (set of missing values) based on $i \in \mathcal{I}$. We construct the vector for the rest of the indexes as $\tilde{\mathbf{Y}}_t$, i.e., based on all $i \notin \mathcal{I}$. Further, we transform all the components to Normal(0, 1) scale by the $\Phi^{-1}(F(Y_{it}; a_i, b_i, c_i))$ transformation. Given that the transformed data follows a multivariate normal distribution, we can simulate the observations corresponding to the missing locations using the standard result of the conditional distribution for multivariate normal vectors and then transform back to the original scale using the Gaussian CDF and the gamma quantile function.

5.2 MCMC implementation

We implement the MCMC algorithm in R (<http://www.r-project.org>). For both simulation studies and the Indian rainfall data application, we draw 200,000 samples from the posterior distribution and discard the first 40,000 observations as burn-in. Further, we perform thinning by 20 iterations and draw inferences based on 8,000 post-burn-in samples from the posterior distribution. For the real data application, where the data includes missing observations at 3 out of 64 years, the computation time is approximately 36 minutes. In the simulation studies, which do not contain any missing data, the computation time is approximately 18 minutes. We perform all the computations on a workstation with an AMD Ryzen 9 5900x processor and 64GB RAM. We monitor the convergence and mixing through Geweke statistics and effective sample sizes [59].

6 Simulation study

We perform a simulation study focusing on the correctness of the estimation procedure detailed in Section 5 and also to study how spatial correlation can effectively help in reducing the uncertainty of the parameter estimates. For each of the three choices of $\rho \in \{0, 0.5, 0.9\}$, representing zero, moderate, and high spatial correlation, we simulate 100 datasets from the proposed model in Section 4.2. Here, we set the true parameter values for \mathbf{a} , \mathbf{b} , and \mathbf{c} to the estimates obtained from the real dataset in Figure 2. Here, we compare models having a CAR structure at the data level and either independence, CAR, or ICAR structure at the prior level. For all values of ρ in the data-generating models, the marginal distribution of the observations remains the same for each region due to choosing the same areally-varying coefficient vectors.

For each model, we compare the Mean Square Errors (MSEs), posterior Standard Deviations (SDs), and Coverage Probabilities (CovPs) of the parameters \mathbf{a} , \mathbf{b} , \mathbf{c} and ρ based on the posterior samples drawn using MCMC. For each of the 100 datasets, we obtain MSEs and posterior SDs for each a_i , b_i , and c_i . Here, we report the average of the MSEs for all 34 a_i s and 100 datasets, for example. For ρ , we report the average of the MSEs for all 100 datasets. We also obtain the SDs reported here via a similar averaging. For calculating CovPs, we first calculate the 95% credible interval for the corresponding parameters and check whether the true value falls within that interval. Thus, we obtain a binary value for each dataset and each i . Further, we average across all 34 regions and 100 datasets for a_i s, b_i s, and c_i s and report the average. For ρ , we only obtain a similar binary value from each dataset and report the average across 100 datasets. We report the results in Table 1. When the true data generating model has $\rho = 0$, we leave the CovPs blank for ρ because the posterior distribution is supported over $(0, 1)$ and does not include zero.

When true $\rho = 0$, comparing all the metrics across models for a_i s, we observe that the CAR-ICAR model provides the smallest MSE, the smallest SD, and the highest CovPs. We observe similar results for b_i s, c_i s, and ρ , indicating that an ICAR prior is more suitable due to the natural spatial pattern of the true areally-varying coefficients obtained from the Indian rainfall dataset. Here, the posterior variances of the parameters ρ_a , ρ_b , and ρ_c are high. Hence, even if an ICAR prior is less flexible (due to fixed spatial autocorrelation one), it provides a better model fitting. When true $\rho = 0.5$, i.e., when the spatial correlation at the data layer is moderate, we see a similar performance comparison for a_i s and b_i s. For c_i s, while the average MSE is the smallest for the CAR-ICAR model, the CAR-Indep model provides the smallest average posterior SD, although comparable with the CAR-ICAR model. For ρ , in terms of MSE, CAR-Indep and CAR-CAR models perform the best jointly, while for the CAR-Indep model, the average posterior SD is the smallest. When true $\rho = 0.9$, i.e., when the spatial correlation at the data layer is strong, the CAR-ICAR and CAR-CAR models usually provide better results for all metrics, except for the low coverage probability (0.9) for ρ in the case of CAR-ICAR and CAR-CAR models. Based on a global comparison with all data-generating scenarios, the CAR-ICAR model is parsimonious and performs equally or better than the alternatives.

Table 1: Average MSE, posterior SD, and coverage probability (CovP) of the areally-varying coefficients and the spatial autocorrelation parameter for independent, CAR, and ICAR priors along with a CAR model specification for the data layer. Here, we consider low through high values of the true spatial autocorrelation parameter and report the results averaged across different regions and 100 simulated datasets (for areally-varying coefficients) and for ρ by averaging across 100 simulated datasets. A smaller MSE and SD value and a higher CovP value are preferred.

		CAR-Indep			CAR-ICAR			CAR-CAR		
		MSE*	SD**	CovP	MSE*	SD**	CovP	MSE*	SD**	CovP
$\rho = 0$	a	48.283	4.405	0.946	43.449	4.164	0.952	44.7	4.244	0.951
	b	1.665	2.791	0.95	1.653	2.784	0.947	1.66	2.787	0.949
	c	1.162	2.31	0.95	1.073	2.203	0.946	1.115	2.278	0.95
	ρ	5.327	4.06	-	5.105	4.005	-	5.185	4.014	-
$\rho = 0.5$	a	46.165	4.32	0.941	41.638	4.106	0.945	42.737	4.176	0.949
	b	1.716	2.789	0.945	1.709	2.785	0.947	1.712	2.788	0.946
	c	1.216	2.272	0.931	1.153	2.273	0.943	1.175	2.295	0.945
	ρ	4.109	4.474	0.94	4.111	4.485	0.96	4.109	4.487	0.96
$\rho = 0.9$	a	40.089	3.991	0.944	37.304	3.867	0.947	37.966	3.904	0.948
	b	1.799	2.783	0.937	1.768	2.779	0.94	1.776	2.78	0.941
	c	1.185	2.24	0.93	1.203	2.403	0.959	1.17	2.339	0.95
	ρ	0.55	1.804	0.94	0.552	1.797	0.9	0.552	1.796	0.9

* multiplied by 1000 for MSE of the parameters **b**, **c** and ρ .

** multiplied by 100 for SD of the parameters **b**, **c** and ρ .

7 Indian rainfall data analysis

We first fit the CAR-Indep, CAR-CAR, and CAR-ICAR models to the Indian rainfall dataset and compare the models based on specific metrics. Here, unlike the simulation settings, the true values of the parameters are not known, and hence, we cannot compare the models in terms of MSEs and coverage probabilities. Hence, we only compare the average posterior SDs for a_i s, b_i s, and c_i s and the posterior SD of ρ . Besides, we compare the DIC and WAIC of the models as described in Section 2.6. We report the results in Table 2. Except for the average posterior SD of c_i s, all other metrics indicate a superior performance of the CAR-ICAR model. Regarding DIC and WAIC, the ICAR prior provides a better fitting and prediction performance than the CAR prior, followed by the independent priors; this result indicates the suitability of allowing spatially-varying coefficients in a Gaussian graphical model framework.

We further consider the CAR-ICAR model only for drawing inferences and report results obtained based on it. To assess the quality of MCMC chains, we use Geweke statistics for the convergence of the post-burn-in samples and the effective number of samples (ESS) for mixing and sample autocorrelation. We report the average of the Geweke statistics and the ESS values for areally-varying coefficients. A high value of ESS is preferred. The Geweke statistic is a z -score; hence, its absolute value being lower than 1.96 indicates the convergence of the MCMC chains. We report the results in Table 3. While the ESS values are relatively higher for all the model hyperparameters, they are usually smaller for the main model parameters **a**, **b**, **c**, and ρ . Overall, the

Table 2: Average Standard deviations of the posterior of the parameters \mathbf{a} , \mathbf{b} , \mathbf{c} and ρ (if applicable), along with model comparison. A smaller value of the metrics indicates a better fitting and prediction performance in a leave-one-out cross-validation.

	$\frac{1}{n} \sum_i sd(a_i)$	$\frac{1}{n} \sum_i sd(b_i)$	$\frac{1}{n} \sum_i sd(c_i)$	$sd(\rho)$	DIC	WAIC
Ind	4.105	2.753	2.077	1.225	28149.7	2235948
ICAR	3.887	2.786	2.293	1.141	28098.7	2201614
CAR	3.983	2.844	2.21	1.198	28128.9	2240857

* multiplied by 100 for the parameters \mathbf{b} , \mathbf{c} and ρ .

ESS values are reasonable for all parameters and hyperparameters. Further, the Geweke statistics for all parameters and hyperparameters are close to zero and not outside the interval ± 1.96 , indicating convergence of the MCMC chains after the burn-in periods. Altogether, both the metrics suggest that the MCMC samples are of reasonably good quality for drawing statistical inferences.

Table 3: Average effective sample size and Geweke statistics of different parameters of the CAR-ICAR model

	\mathbf{a}	\mathbf{b}	\mathbf{c}	ρ	μ_a	μ_b	μ_c	σ_a^2	σ_b^2	σ_c^2
ESS	521	169	186	180	8000	8000	7718	1726	8000	820
Geweke	-0.52	0.65	0.73	0.32	-1	0.16	-0.19	-0.75	1.11	-0.07

We report the posterior means and SDs of a_i s, b_i s, and c_i s in Figure 3. Besides, the posterior mean and SD of ρ are 0.9309 and 0.0114, respectively. The spatial patterns of the coefficients are similar to the ones observed in Figure 2, which indicates that the CAR-ICAR model can capture the spatial patterns of the coefficients correctly. The posterior means of a_i s, i.e., the shape parameters of the gamma model, are higher in the middle, eastern, and southern parts of India. At the same time, they are low in the northwestern parts of India and also near the northeastern meteorological subdivisions. Some eastern and western Indian subdivisions showcase higher posterior SD than others. The posterior means of b_i s, the intercept-related parameters of the gamma model, are higher in the northwestern and northeastern meteorological subdivisions. At the same time, they are lowest in the middle parts of the country. Finally, a positive c_i indicates a negative trend follows from (10). We observe positive estimates of c_i s throughout the country, indicating a negative trend in the amount of annual total rainfall. However, due to high posterior SDs, most of these estimates are insignificant except for three meteorological subdivisions: 1. Arunachal Pradesh, 2. Assam and Meghalaya, and 3. Nagaland, Manipur, Mizoram, and Tripura. A significantly negative trend for these Himalayan regions indicates a mean annual total rainfall decline and thus requires further environmental assessment.

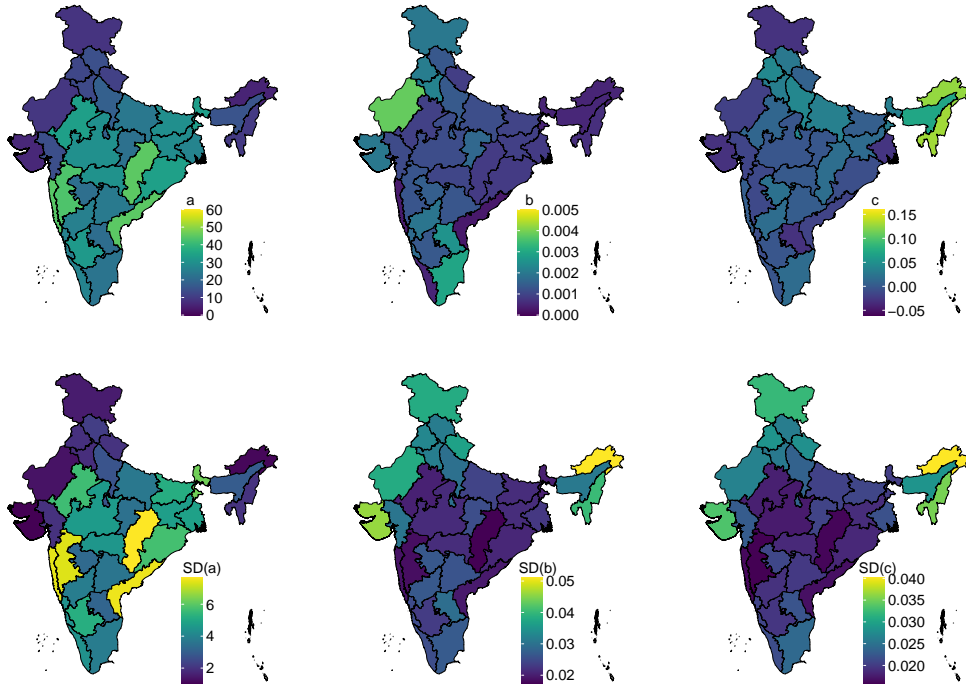


Fig. 3: Posterior means (top) and SDs (bottom) of a_i s, b_i s, and c_i s based on fitting the CAR-ICAR model.

8 Concluding remarks

Evaluating the availability of rainfall water is essential for rainfed agriculture, which is predominantly practiced in India. Considering potential trends in rainfall patterns due to climate change, we develop a statistical model to analyze annual total rainfall data for 34 meteorological subdivisions of mainland India from 1951 to 2014. Our approach models the marginal distributions using a gamma regression model while capturing dependence through a Gaussian conditional autoregressive (CAR) copula model. Given the natural variation in average annual rainfall across the country's diverse climatic regions, we incorporate areally-varying gamma regression coefficients within a latent Gaussian model framework. The dependence structure in both the likelihood and prior layers is governed by the neighborhood relationships of the regions, where we examine both CAR and intrinsic CAR structures for the priors. We employ Markov chain Monte Carlo algorithms to facilitate Bayesian inference, precisely a combination of block Metropolis-Hastings and single-component Metropolis-Hastings steps within a Gibbs sampler. Additionally, the proposed methodology effectively imputes missing data within the Gibbs sampling. Our model demonstrates superior performance in simulation studies compared to alternatives that do not account for dependence structures in the data or prior layers. Applying our methodology to the Indian areal rainfall dataset, we estimate model parameters, correctly quantify the uncertainties,

and investigate the potential impact of climate change on rainfall patterns across India. The mean annual rainfall shows a significant negative trend for three meteorological subdivisions of northeastern India.

A drawback of the proposed methodology is a specific dependence structure across space determined by the neighborhood structure of India’s meteorological subdivisions. The literature contains a large number of copula models for Gaussian graphical models. However, our approach is parsimonious and implementable in all scenarios where a CAR model is applicable. The significance of our proposed methodology extends beyond rainfall modeling. It provides a generalizable framework for analyzing other spatially dependent climatic variables, such as temperature and humidity, which exhibit complex dependence structures. This approach is instrumental in climate impact assessments, where accurate predictions of future rainfall trends can inform adaptation and mitigation strategies [60]. Incorporating spatially varying coefficients (SVCs) into rainfall modeling is crucial for accurately capturing the inherent heterogeneity of precipitation patterns across different regions. Traditional models with fixed coefficients often fail to account for local variations, leading to oversimplified representations of rainfall processes. Allowing model parameters to change spatially enables SVC models to represent better the complex interactions between environmental factors and rainfall distribution. This enhanced flexibility improves the precision of hydrological predictions, which is vital for effective water resource management and flood risk assessment. For instance, studies have demonstrated that SVC models can effectively capture both short-range and long-range spatial dependencies in hydrological processes, leading to more accurate estimations of mean annual runoff coefficients [45, 61, 62]. Integrating SVCs into rainfall models allows for a more nuanced understanding of spatial variability, leading to more reliable and region-specific hydrological insights.

Acknowledgement

The authors would like to thank Aritra Basak for providing some codes for preliminary analysis and the adjacency matrix used in our paper. The research of the second author is supported by the Start-up Research Grant (SRG), Science and Engineering Research Board, Department of Science & Technology, Government of India, with Award No. SERB-MATH-2023632.

Supplementary information

Codes (written in R) for implementing our proposed methodology and the dataset analyzed in this paper are provided in the Supplementary Material.

Disclosure statement

No potential conflict of interest was reported by the authors.

References

- [1] Venkateswarlu, B.: Rainfed agriculture in India: Issues in technology development and transfer, impact of climate change in rainfed agriculture and adaptation strategies. Hyderabad, India: DRIDA (2011)
- [2] Hazra, A., Ghosh, A.: Robust statistical modeling of monthly rainfall: The minimum density power divergence approach. *Sankhya B* **86**(1), 241–279 (2024)
- [3] Allan, R.P., Arias, P.A., Berger, S., Canadell, J.G., Cassou, C., Chen, D., Cherchi, A., Connors, S.L., Coppola, E., Cruz, F.A., *et al.*: Intergovernmental panel on climate change (IPCC). Summary for policymakers. In: *Climate Change 2021: The Physical Science Basis. Contribution of the Working Group I to the Sixth Assessment Report of the Intergovernmental Panel on Climate Change*, pp. 3–32. Cambridge University Press, Cambridge (2023)
- [4] Guhathakurta, P., Rajeevan, M.: Trends in the rainfall pattern over India. *International Journal of Climatology: A Journal of the Royal Meteorological Society* **28**(11), 1453–1469 (2008)
- [5] Hazra, A., Huser, R., Bolin, D.: Efficient modeling of spatial extremes over large geographical domains. *Journal of Computational and Graphical Statistics*, 1–17 (2024)
- [6] Todorovic, P., Woolhiser, D.A.: A stochastic model of n -day precipitation. *Journal of Applied Meteorology* **14**(1), 17–24 (1975)
- [7] Hazra, A., Bhattacharya, S., Banik, P.: A Bayesian zero-inflated exponential distribution model for the analysis of weekly rainfall of the eastern plateau region of India. *Mausam* **69**(1), 19–28 (2018)
- [8] Barger, G.L., Thom, H.C.: Evaluation of drought hazard. *Agronomy Journal*, 519–526 (1949)
- [9] Mooley, D.A., Crutcher, H.L.: An Application of the Gamma Distribution Function to Indian Rainfall. ESSA Technical Report, U.S. Dept. of Commerce, EDS, Methuen, London (1968)
- [10] Kwaku, X.S., Duke, O.: Characterization and frequency analysis of one day annual maximum and two to five consecutive days maximum rainfall of Accra, Ghana. *ARNP J. Eng. Appl. Sci* **2**(5), 27–31 (2007)
- [11] Mandal, S., Choudhury, B.: Estimation and prediction of maximum daily rainfall at Sagar Island using best fit probability models. *Theoretical and Applied Climatology* **121**(1), 87–97 (2015)
- [12] Duan, J., Sikka, A.K., Grant, G.E.: A comparison of stochastic models for generating daily precipitation at the HJ Andrews Experimental Forest. *Northwestern*

- Science **69**(4) (1995)
- [13] Lana, X., Serra, C., Casas-Castillo, M., Rodríguez-Solà, R., Redaño, A., Burgueño, A.: Rainfall intensity patterns derived from the urban network of Barcelona (NE Spain). *Theoretical and Applied Climatology*, 1–19 (2017)
 - [14] Madi, M.T., Raqab, M.Z.: Bayesian prediction of rainfall records using the generalized exponential distribution. *Environmetrics* **18**(5), 541–549 (2007)
 - [15] Hazra, A.: Minimum density power divergence estimation for the generalized exponential distribution. *Communications in Statistics-Theory and Methods* **54**(4), 1050–1070 (2025)
 - [16] Martinez-Villalobos, C., Neelin, J.D.: Why do precipitation intensities tend to follow gamma distributions? *Journal of the Atmospheric Sciences* **76**(11), 3611–3631 (2019)
 - [17] Nelder, J.A., Wedderburn, R.W.: Generalized linear models. *Journal of the Royal Statistical Society Series A: Statistics in Society* **135**(3), 370–384 (1972)
 - [18] Amin, M., Qasim, M., Amanullah, M., Afzal, S.: Performance of some ridge estimators for the gamma regression model. *Statistical papers* **61**, 997–1026 (2020)
 - [19] Diggle, P.J., Tawn, J.A., Moyeed, R.A.: Model-based geostatistics. *Journal of the Royal Statistical Society Series C: Applied Statistics* **47**(3), 299–350 (1998)
 - [20] Sklar, A.: Distribution functions of n dimensions and margins. *Publications of the Institute of Statistics of the University of Paris* **8**(229), 31 (1959)
 - [21] Nelsen, R.B.: *An Introduction to Copulas*. Springer, New York (2006)
 - [22] Chen, L., Guo, S., *et al.*: *Copulas and Its Application in Hydrology and Water Resources*. Springer, Singapore (2019)
 - [23] Frees, E.W., Valdez, E.A.: Understanding relationships using copulas. *North American Actuarial Journal* **2**(1), 1–25 (1998)
 - [24] Omid, M., Mohammadzadeh, M.: Spatial interpolation using copula for non-Gaussian modeling of rainfall data. *Journal of The Iranian Statistical Society* **17**(2), 165–179 (2022)
 - [25] Sang, H., Gelfand, A.E.: Continuous spatial process models for spatial extreme values. *Journal of Agricultural, Biological, and Environmental Statistics* **15**, 49–65 (2010)
 - [26] Huser, R., Genton, M.G.: Non-stationary dependence structures for spatial extremes. *Journal of Agricultural, Biological, and Environmental Statistics* **21**,

470–491 (2016)

- [27] Gräler, B., Pebesma, E.: The pair-copula construction for spatial data: a new approach to model spatial dependency. *Procedia Environmental Sciences* **7**, 206–211 (2011)
- [28] Okhrin, O., Ristig, A., Xu, Y.-F.: Copulae in high dimensions: an introduction. *Applied Quantitative Finance*, 247–277 (2017)
- [29] Nazeri Tahroudi, M., Ramezani, Y., Michele, C., Mirabbasi, R.: Multivariate analysis of rainfall and its deficiency signatures using vine copulas. *International Journal of Climatology* **42**(4), 2005–2018 (2022)
- [30] Nazeri Tahroudi, M., Ramezani, Y., De Michele, C., Mirabbasi, R.: Application of copula-based approach as a new data-driven model for downscaling the mean daily temperature. *International Journal of Climatology* **43**(1), 240–254 (2023)
- [31] Zhang, L., Singh, V.P.: Bivariate rainfall and runoff analysis using entropy and copula theories. *Entropy* **14**(9), 1784–1812 (2012)
- [32] Najjari, V., Unsal, M.: An application of Archimedean copulas for meteorological data. *Gazi University Journal of Science* **25**(2), 417–424 (2012)
- [33] Zhang, L., Singh, V.P.: Bivariate rainfall frequency distributions using Archimedean copulas. *Journal of Hydrology* **332**(1-2), 93–109 (2007)
- [34] Mesbahzadeh, T., Miglietta, M., Mirakbari, M., Soleimani Sardoo, F., Abdolhosseini, M.: Joint modeling of precipitation and temperature using copula theory for current and future prediction under climate change scenarios in arid lands (Case Study, Kerman Province, Iran). *Advances in Meteorology* **2019**(1), 6848049 (2019)
- [35] Musgrove, D., Hughes, J., Eberly, L.E.: Hierarchical copula regression models for areal data. *Spatial Statistics* **17**, 38–49 (2016)
- [36] Khan, F., Spöck, G., Pilz, J.: A novel approach for modelling pattern and spatial dependence structures between climate variables by combining mixture models with copula models. *International Journal of Climatology* **40**(2), 1049–1066 (2020)
- [37] Lee, T.: Multisite stochastic simulation of daily precipitation from copula modeling with a gamma marginal distribution. *Theoretical and Applied Climatology* **132**, 1089–1098 (2018)
- [38] Berg, M., Vandenberghe, S., De Baets, B., Verhoest, N.: Copula-based downscaling of spatial rainfall: a proof of concept. *Hydrology and Earth System Sciences* **15**(5), 1445–1457 (2011)

- [39] Baxevani, A., Lennartsson, J.: A spatiotemporal precipitation generator based on a censored latent Gaussian field. *Water Resources Research* **51**(6), 4338–4358 (2015)
- [40] Besag, J.: Spatial interaction and the statistical analysis of lattice systems. *Journal of the Royal Statistical Society: Series B (Methodological)* **36**(2), 192–225 (1974)
- [41] Cliff, A.D., Ord, J.K.: *Spatial Processes: Models and Applications*. Pion Ltd., London (1981)
- [42] Banerjee, S., Carlin, B.P., Gelfand, A.E.: *Hierarchical Modeling and Analysis for Spatial Data*. CRC press, Boca Raton, US (2015)
- [43] Villarini, G., Smith, J.A., Serinaldi, F., Ntelekos, A.A.: On the stationarity of annual flood peaks in the continental United States during the 20th century. *Water Resources Research* **46**(8) (2010)
- [44] Cressie, N., Wikle, C.K.: *Statistics for Spatio-temporal Data*. John Wiley & Sons, Hoboken, New Jersey (2011)
- [45] Gelfand, A.E., Kim, H.-J., Sirmans, C., Banerjee, S.: Spatial modeling with spatially varying coefficient processes. *Journal of the American Statistical Association* **98**(462), 387–396 (2003)
- [46] Mollié, A.: Bayesian mapping of disease. In: Gilks, W.R., Richardson, S., Spiegelhalter, D.J. (eds.) *Markov Chain Monte Carlo in Practice*, pp. 359–379. Chapman and Hall, London (1996)
- [47] Fernández-Rasines, M., Gutiérrez-Peña, J.M.: Bayesian analysis of conditional autoregressive models. *Annals of the Institute of Statistical Mathematics* **62**, 103–121 (2010)
- [48] Lee, D., Sahu, S.K.: A Bayesian localized conditional autoregressive model for estimating the health effects of air pollution. *Bayesian Analysis* **10**(1), 235–258 (2015)
- [49] Lee, D., Napier, F.D.: Spatio-temporal areal unit modeling in R with conditional autoregressive priors. *Journal of Statistical Software* **84**(9), 1–25 (2017)
- [50] Brook, D.: On the distinction between the conditional probability and the joint probability approaches in the specification of nearest-neighbour systems. *Biometrika* **51**(3/4), 481–483 (1964)
- [51] Ross, S.M.: *Simulation*, 2nd edn. *Statistical Modeling and Decision Science*, p. 282. Academic Press, Inc., San Diego, CA (1997)
- [52] Hazra, A., Reich, B.J., Staicu, A.-M.: A multivariate spatial skew-t process

- for joint modeling of extreme precipitation indexes. *Environmetrics* **31**(3), 2602 (2020)
- [53] Moran, P.A.P.: Notes on continuous stochastic phenomena. *Biometrika* **37**(1/2), 17–23 (1950) <https://doi.org/10.2307/2332142>
- [54] Spiegelhalter, D.J., Best, N.G., Carlin, B.P., Van Der Linde, A.: Bayesian measures of model complexity and fit. *Journal of the royal statistical society: Series b (statistical methodology)* **64**(4), 583–639 (2002)
- [55] Watanabe, S., Opper, M.: Asymptotic equivalence of bayes cross validation and widely applicable information criterion in singular learning theory. *Journal of machine learning research* **11**(12) (2010)
- [56] Vehtari, A., Gelman, A., Gabry, J.: Practical Bayesian model evaluation using leave-one-out cross-validation and WAIC. *Statistics and Computing* **27**(5), 1413–1432 (2017)
- [57] Guhathakurta, P., Sreejith, O., Menon, P.: Impact of climate change on extreme rainfall events and flood risk in India. *Journal of Earth System Science* **120**, 359–373 (2011)
- [58] Freni-Sterrantino, A., Ventrucci, M., Rue, H.: A note on intrinsic conditional autoregressive models for disconnected graphs. *Spatial and Spatio-temporal Epidemiology* **26**, 25–34 (2018)
- [59] Reich, B.J., Ghosh, S.K.: *Bayesian Statistical Methods*. Chapman and Hall/CRC, Boca Raton, USA (2019)
- [60] Fischer, E.M., Beyerle, U., Knutti, R.: Robust spatially aggregated projections of climate extremes. *Nature Climate Change* **3**(12), 1033–1038 (2013)
- [61] Bakar, K.S.: Interpolation of daily rainfall data using censored Bayesian spatially varying model. *Computational Statistics* **35**(1), 135–152 (2020)
- [62] Arnaud, P., Bouvier, C., Cisneros, L., Dominguez, R.: Influence of rainfall spatial variability on flood prediction. *Journal of Hydrology* **260**(1-4), 216–230 (2002)